Dalton Transactions

Accepted Manuscript

ROYAL SOCIETY OF CHEMISTRY

www.rsc.org/dalton

A real-time fluorescent sensor specific to Mg^{2+}: crystallographic evidence, DFT calculation and its use for quantitative determination of magnesium in drinking water†

Guangwen Men, Chunrong Chen, Shitong Zhang, Chunshuang Liang, Ying Wang, Mengyu Deng, Hongxing Shang, Bing Yang and Shimei Jiang*

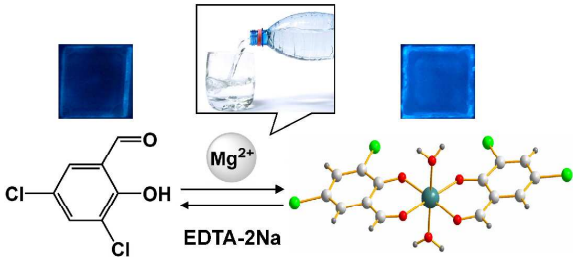

An "off-the-shelf" fluorescence "turn-on" Mg^{2+} chemosensor **BCSA** has been developed for real-time quantitative monitoring of magnesium in drinking water.

Cite this: DOI: 10.1039/c0xx00000x

www.rsc.org/xxxxxx

ARTICLE TYPE

A real-time fluorescent sensor specific to Mg^{2+}: crystallographic evidence, DFT calculation and its use for quantitative determination of magnesium in drinking water†

Guangwen Men, Chunrong Chen, Shitong Zhang, Chunshuang Liang, Ying Wang, Mengyu Deng, Hongxing Shang, Bing Yang and Shimei Jiang*

Received (in XXX, XXX) Xth XXXXXXXXX 20XX, Accepted Xth XXXXXXXXX 20XX
DOI: 10.1039/b000000x

An "off-the-shelf" fluorescence "turn-on" Mg^{2+} chemosensor 3, 5-dichlorosalicylaldehyde (**BCSA**) was rationally designed and developed. This proposed sensor works based on Mg^{2+}-induced formation of the 2:1 **BCSA**-Mg^{2+} complex. The coordination of **BCSA** to Mg^{2+} increases its structural rigidity generating a chelation-enhanced fluorescence (**CHEF**) effect which was confirmed by single crystal XRD studies of the **BCSA**-Mg^{2+} complex and TD/DFT calculation. This sensor exhibits high sensitivity and selectivity for the quantitative monitoring of Mg^{2+} with a wide detection range (0-40 μM), a low detection limit (2.89×10^{-7} mol/L) and a short response time (< 0.5 s). It can also resist the interference from the other co-existing metal ions especially Ca^{2+}. Consequently, this fluorescent sensor can be utilized to monitor Mg^{2+} in real-time within actual samples from drinking water.

Introduction

Magnesium ion, one of the most abundant intracellular divalent cations, has been recognized as a vital biological ion for all living things over the past century.[1] It plays an essential role in many biological processes.[2] From a health point of view, the daily intake of magnesium for an adult human should reach ca. 300 mg, which may come from green vegetables, dairy products, grain and seafood.[3] Deficiencies or excesses of intake of this ion can lead to a variety of diseases.[3, 4] Mineral drinking water may also supply magnesium in fair quantities.[5] The standard method for the determination of Mg^{2+} in drinking water is EDTA complexiometric titration.[6, 7] However, sometimes this method is laborious, time-consuming, reagent-consuming, and poorly removes of the interference from several metal ions. In this regard, the development of reliable and sensitive analytical methods for Mg^{2+} is highly desirable.

Recently, fluorescent chemosensors appear to be particularly attractive on account of their highly sensitive and selective, easy to fabricate and non-destructive properties as well as their capability of remote and in situ monitoring of optical measurement.[8] Tremendous amounts of effort have been put forth for the development of the new fluorescent sensors for metal ions during the past few decades.[8a, 9] Compared to several transition metal ions, such as Hg^{2+}, Cu^{2+} and Zn^{2+},[10] only a few fluorescent chemosensors have been developed for the detection of Mg^{2+} due to its spectroscopic silence.[11] Generally, previous designs for Mg^{2+} fluorescent sensors are based on several metal chelating structures that have a high affinity toward Mg^{2+}; these sensors include β-diketone,[11e] crown ether,[11c, 12] polyether,[13] calix[4]arene,[14] carboxylic acid,[11b] salicylaldehyde Schiff base,[15] etc. However, these synthetic fluorescent sensors demand long preparation time and high cost of synthesis. As an improvement, salicylaldehyde derivatives would be better for the design of Mg^{2+} sensors because they could not only chelate various metal ions accompanied by the spectroscopic changes but also be purchased from commercial source without further synthesis. But, until now, fluorescent Mg^{2+} sensors based on salicylaldehyde derivatives have not been reported.

On the other hand, it is known that the most important feature of the Mg^{2+} sensors is their potential application in the field of quantitative Mg^{2+} discrimination in drinking water. Such Mg^{2+} sensors require high selectivity toward the analyte over the other co-existing species. Most of the reported Mg^{2+} sensors are limited in distinguishing Mg^{2+} from large quantities of Ca^{2+} owing to the similar chemical properties of Mg^{2+} and Ca^{2+} [16] and few examples providing selectivity in Mg^{2+} recognition have been reported.[15a] However, to the best of our knowledge, there is still a research bottleneck with regard to the development of designing highly selective Mg^{2+} fluorescent sensors in practical applications, particularly for the quantitative detection of Mg^{2+} in drinking water.

Herein, we have developed a fluorescence "turn-on" Mg^{2+} sensor based on a simple commercial 3, 5-dichlorosalicylaldehyde **BCSA** (Chart 1). As expected, upon adding Mg^{2+}, the 2:1 **BCSA**-Mg complex producing light blue fluorescence was formed and the emission spectra underwent an obvious blue-shift and an enhancement. According to this significant fluorescence signal change, **BCSA** could detect Mg^{2+} sensitively, selectively and quantitatively with a wide detection range (0-40 μM), a low detection limit (2.89×10^{-7} mol/L) and a short response time (< 0.5 s). Moreover, it could resist the

interference from the other co-existing metal ions especially Ca^{2+}. These results made the application of the quantitative and real-time detection of Mg^{2+} in drinking water a reality. In order to facilitate the applications in portable field analysis for **BCSA**, the PMMA thin film doped with **BCSA** molecules were fabricated and used to monitor Mg^{2+} in drinking water selectively.

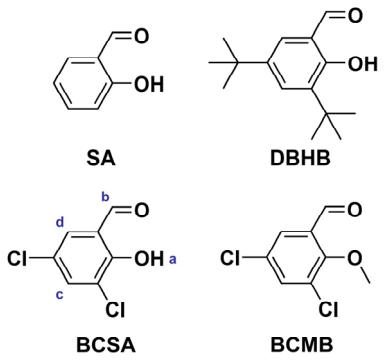

Chart 1. Chemical structures of **SA, DBHB**, **BCSA** and **BCMB**.

Results and discussion

Rational design of the Mg^{2+} sensor based on salicylaldehyde derivatives and its spectral properties.

Compared to the well developed salicylaldehyde Schiff base chemosensors, [17] their simple precursor salicylaldehyde derivatives have rarely been used in the field of metal ions detection through the chelation of its carbonyl O and phenol O[9b]. This is probably due to the weak binding constants and poor optical properties for their metal complexes. These factors are known to be readily influenced by substituents on the benzene ring of salicylaldehyde derivatives. In this regard, the following simple, commercial compounds were selected: non-substituted **SA**, **DBHB** substituted by 3, 5-position tert-butyl groups, and **BCSA** substituted by 3, 5-position chlorine atoms (Chart 1). These compounds were subjected to examine their responses to different metal ions (Fig. S1, ESI†). The results showed no fluorescent emission for **SA** in the fluorescence spectra. However, this compound displayed a weak fluorescent emission after the addition of Al^{3+} (Fig. S1c, ESI†). These observations are similar to those reported by Wu et al.[9b] Both **DBHB** involving electron donating groups and its mixture solutions with different metal ions showed no fluorescence (Fig. S1b, ESI†). While **BCSA** involving electron withdrawing groups in 3, 5-position substituents on the phenol group exhibited a fluorescent emission at 509 nm and it could selectively respond to Mg^{2+} based on a strong light blue emission (Fig. S1a, ESI†). These results indicated that 3, 5-position substituents on the phenol group not only distinctly affected the fluorescence intensities of salicylaldehyde derivatives and their metal complex,[17a, 18a] but also determined the types of the analytes. This was because the dichloro-substitution increased acidity of the phenolic part of **BCSA**[18b] and thereby promoted the deprotonated process after which phenol O takes part in metal ion binding. On the basis of its excellent selectivity, **BCSA** was selected as a candidate for Mg^{2+} chemosensor. In order to further study the structural contribution of 2-hydroxy group to Mg^{2+} binding, **BCMB** in which the involved proton was substituted by a methyl group was designed (Chart 1). Unlike **BCSA**, there was no obvious change in the fluorescence spectra of **BCMB** after adding different metal ions including Mg^{2+} (Fig. S1d, ESI†). The main reason is the existence of 2-methoxy group prevents **BCMB** from the deprotonated process. Hence, in this work, we preferred **BCSA** as a Mg^{2+} fluorescent sensor and tried to explore its Mg^{2+} detection properties, mechanisms and applications.

Mg^{2+} detection properties of BCSA.

According to previous works, [19] salicylaldehyde derivatives exist as intramolecular hydrogen-bonded, closed conformers in non-polar solvents. Whereas in polar protic solvents that can break the intramolecular hydrogen bond of the closed conformer, the strongly solvated open conformers are dominant. Hydroxyl derivatives of aromatic compounds are generally acidic in the excited singlet state relative to the ground state.[20] Therefore, there is a tendency for **BCSA** in the excited state to undergo intermolecular proton transfer with the polar protic solvent (Scheme 1); the resulting deprotonated form of **BCSA** could possibly show a large Stokes-shifted emission.[21]

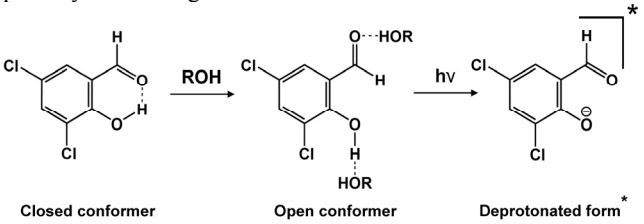

Scheme 1. The ground state reaction and photochemical scheme of **BCSA** in polar protic solvents.

In order to satisfy actual application, the sensor **BCSA** was used in the HEPES buffer-ethanol solution; hence it exists predominantly in its open conformer of the enol form in the ground state. In this solution, **BCSA** shows a single large Stokes-shifted emission band centered at 509 nm with a relatively low quantum yield (Φ_f) of 0.018. So this fluorescence band mainly belongs to the emission of the deprotonated form of **BCSA** (Fig. 1a). Gradual titration of Mg^{2+} led to a large increase in the intensity of the emission as the fluorescence peak underwent a 28 nm blue shift from 509 to 481 nm. The intensity of the fluorescence peak had a 22-fold enhancement and a high quantum yield of 0.333 whenever the solution was saturated with ~3 equiv. Mg^{2+}. As a result, the fluorescent color of the solution turned from green to light blue (inset in Fig. 1a). This is presumably attributed to the formation of the **BCSA**-Mg^{2+} complex which causes a chelation-enhanced fluorescence (**CHEF**) effect.[15c, 22]

More interestingly, it can be noticed that the increasing fluorescence intensity of **BCSA** had a significant linear correlation with the concentration of Mg^{2+} over a wide range of 0-40 μM (Fig. 1b). Hence, **BCSA** can accomplish the quantitative analysis of Mg^{2+}, and its wide detection range makes it possible to meet more requirements in practical applications. The detection limit of **BCSA** calculated as 2.89×10^{-7} mol/L from the fluorescence titration spectra.[23] This result indicates that the proposed fluorescence turn-on sensor shows quite high sensitivity

toward trace amounts of Mg^{2+} compared to those of some previously reported Mg^{2+} sensors.[14b, 15b]

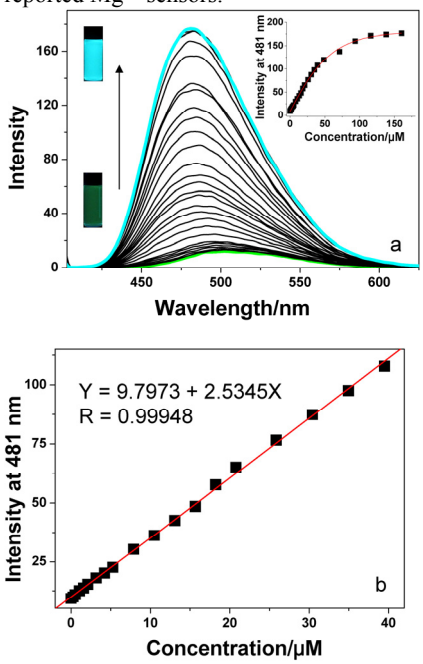

Fig. 1 (a) Fluorescence spectra of **BCSA** in a 95:5 (v/v) ethanol-HEPES (0.05 M, pH = 7.0) solution upon addition of increasing concentration of Mg^{2+} (λ_{ex} = 400 nm, [**BCSA**] = 50 μM). The inset is a plot of intensity change vs. concentration of Mg^{2+} added. (b) The fluorescence intensity at 481 nm of **BCSA** (50 μM) was linearly related to the concentration of Mg^{2+} (0-40 μM).

The response of **BCSA** to Mg^{2+} was confirmed to be reversible according to the titration of the Mg^{2+} bonding agent, EDTA disodium (Fig. S3, ESI†). The addition of EDTA disodium to the mixture of **BCSA** and Mg^{2+} solution resulted in a reduction of the emission and a regeneration of free **BCSA**. The reversibility is beneficial to the fabrication of reusable devices for sensing Mg^{2+}. These observations demonstrate **BCSA** to be a reversible high-performance Mg^{2+} chemosensor with a fluorescence turn-on signaling. Moreover, Fig. S4 depicts the fluorescence intensity changes of the bands of **BCSA** and **BCSA**-Mg^{2+} at 481 nm in different organic solvents-HEPES solutions. It is obvious that the fluorescent response of **BCSA** to Mg^{2+} happened in all these solvents. The results above manifest that this sensor can sensitively detect Mg^{2+} in different water miscible organic solutions.

To evaluate the selectivity of **BCSA** in practice, changes of the fluorescence intensity at 481 nm of **BCSA** caused by Mg^{2+} and some other metal ions including alkali, alkaline earth, and transition metal ions under the same conditions were investigated. As shown in Fig. 2a, only Mg^{2+} led to a prominent fluorescence enhancement, while the other ions did not cause obvious interference. It is worth mentioning that except for Zn^{2+} and Ca^{2+}, the other competitive metal ions displayed no further increase of emission intensity other than a certain extent quenching of the fluorescence of **BCSA**. Meanwhile, the titration of Mg^{2+} caused a 22-fold fluorescence enhancement that was approximately 9 times larger than the value induced by an equivalent addition of Zn^{2+} and 20 times larger than that of Ca^{2+}. These results indicate that **BCSA** can easily distinguish Mg^{2+} from other cations according to fluorescence spectroscopy. From the practical point of view, we conducted competitive experiments at the proper concentration level (mg/L) close to that of real samples in commercial mineral drinking water. Negligible interference to the Mg^{2+} sensing was brought by the introduction of Zn^{2+}, Ca^{2+}, K^+, Li^+, Na^+, Sr^{2+}, Ba^{2+} and NH_4^+ cations (Fig. 2b). Evidently, **BCSA** exhibits excellent interference immunity to the common mineral cations in drinking water, which is comparable with previous fluorescent Mg^{2+} sensors.[11f, 12a, 12b, 13, 14a]

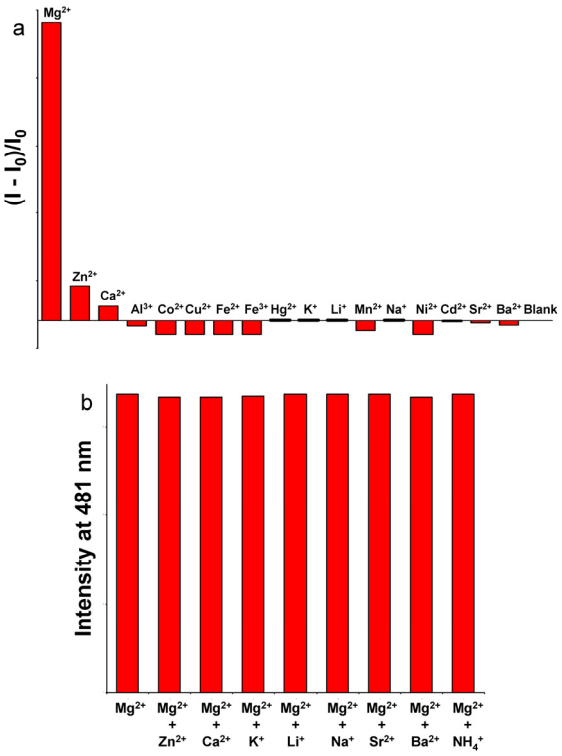

Fig. 2 (a) $(I-I_0)/I_0$ ratios of **BCSA** (50 μM) in the presence of 8 equiv. of various metal ions in a 95:5 (v/v) ethanol-HEPES (0.05 M, pH = 7.0) solution. (b) Fluorescence intensity of **BCSA**-Mg^{2+} in the presence of other competing metal ions in a 95:5 (v/v) ethanol-HEPES buffer solution. The concentration of **BCSA** was 50 μM, while that of Mg^{2+} and other cations were 10 mg/L ([Ca^{2+}] = 30 mg/L) in HEPES buffer (0.05 M, pH = 7.0), respectively (λ_{ex} = 400 nm).

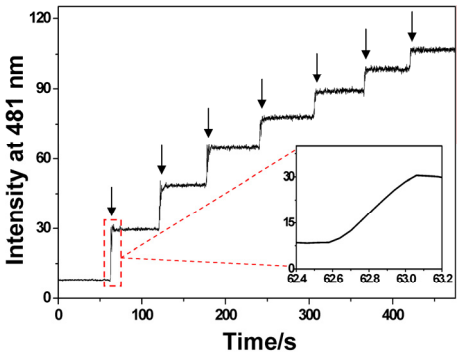

Fig. 3 Time course of the fluorescence response of **BCSA** (50 μM) to Mg^{2+}; arrows represent addition of the equivalent Mg^{2+}. Inset: The magnification of the region between 62.4 and 63.2 s (λ_{ex} = 400 nm).

In addition, a short response time is necessary for a fluorescent chemosensor to monitor Mg^{2+} in real samples. So we also carried out the time course of the response for **BCSA** to successive addition of the equivalent Mg^{2+} (Fig. 3). Excitingly, we found the response was extremely rapid and completed in less than 0.5 s (inset in Fig. 3). Therefore, **BCSA** is likely to be used for the real-time detection of Mg^{2+} because it and its immobilization materials can be applied to in-situ, fast detection in drinking water.

Mechanisms of Mg^{2+} detection.

First, a preliminary explanation of the sensing mechanism was investigated by the UV-vis spectroscopic titration method. In the absorption spectra of **BCSA**, the maximum long-wave absorption band in the range 300-395 nm that centers at 341 nm is assigned to a $S_0 \rightarrow {}^1\pi\pi^*$ transition absorption and its shoulder absorption band around 400 nm may be owing to the ground state intermolecular hydrogen bonding between solute and solvent interaction[19, 21] (Fig. 4a). Upon the addition of increasing concentrations of Mg^{2+}, the original absorption band at 341 nm decreased and the absorption band centered at 400 nm enhanced gradually. The changes in UV-vis absorption spectra induced by Mg^{2+} are probably due to the coordination interaction between **BCSA** and Mg^{2+} ion.

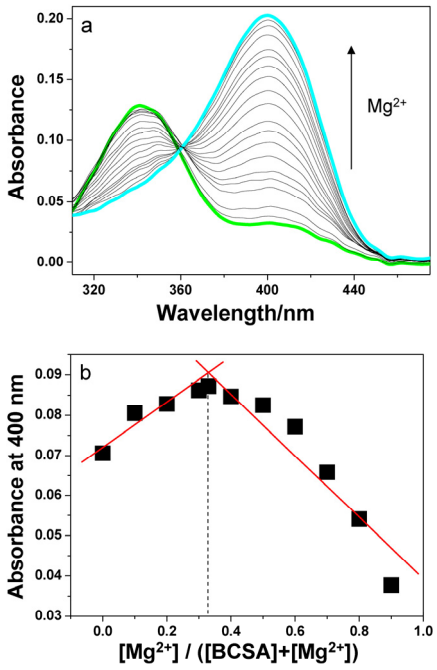

Fig. 4 (a) The absorption spectra of probe **BCSA** (50 μM) in a 95:5 (v/v) ethanol-HEPES (0.05 M, pH = 7.0) solution upon addition of increasing concentrations of Mg^{2+} (0-400 μM). (b) Absorbance changes of band at 400 nm of **BCSA** and Mg^{2+} with a total concentration of 50 μM in a 95:5 (v/v) ethanol-HEPES (0.05 M, pH = 7.0) solution, indicating a 2:1 stoichiometric ratio of **BCSA**:Mg^{2+}.

The mode of coordination of **BCSA** with Mg^{2+} was revealed by the continuous variation (Job's plot, Fig. 4b) analysis of the absorption spectra, which showed a maximum at 0.33 mole fraction of Mg^{2+}. This proved the formation of a 2:1 stoichiometric compexation of **BCSA** with Mg^{2+}. More direct evidence was provided by comparing the ESI mass spectra of **BCSA** and **BCSA**-Mg^{2+}. In absence of Mg^{2+}, a peak at m/z = 188.9 corresponding to [**BCSA**-H]$^-$ in the ESI mass spectrum under negative ion mode was clearly observed (Fig. S5, ESI†). While adding 4 equiv. Mg^{2+}, the formation of 2:1 complex between **BCSA** and Mg^{2+} was further confirmed by the emergence of the peaks at m/z = 494.1 attributed to [2**BCSA**+$MgCl_2$+Na]$^+$ (Fig. S6, ESI†) and m/z = 474.7 attributed to [2**BCSA**+$MgCl_2$]$^-$ (Fig. S7, ESI†) in the ESI mass spectra under positive and negative ion modes, respectively.

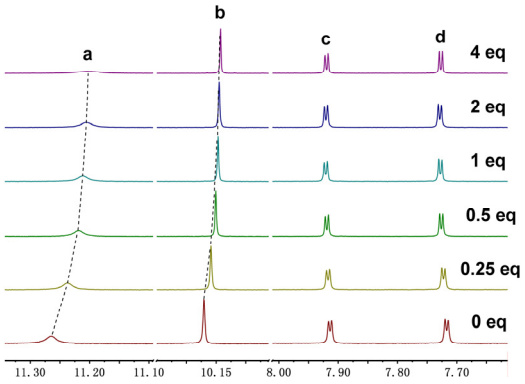

Fig. 5 Partial ^{1}H NMR spectra of **BCSA** (5mM in DMSO-d_6) in the presence of increasing equivalents of Mg^{2+}.

Further efforts were put forth to study the interaction of **BCSA** with Mg^{2+} by means of the ^{1}H NMR titration experiment (Fig. 5). With the addition of excess Mg^{2+}, the signal of the hydroxyl proton H_a experienced an obvious upfield shift from 11.26 to 11.19 ppm and a decrease in intensity. This observation was due to the coordination between Mg^{2+} and 2-hydroxy O atom of **BCSA** with the deprotonation of the phenolic hydroxyl group. At the same time, the aldehyde proton H_b at 10.16 ppm was shifted upfield toward 10.13 ppm, indicating the involvement of the carbonyl O. These data give the conclusion that the binding of **BCSA** to Mg^{2+} generates a rigid structure through a chelating reaction via the carbonyl O and phenol O.

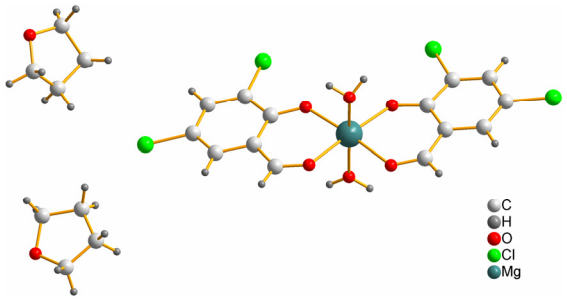

Fig. 6 The crystal structure of the compound **BCSA**-Mg^{2+}. One part of disordered THF molecule is omitted for clarity.

Light yellow-colored, strong blue fluorescent crystals were formed after slow evaporation of solvent from the sample that contained **BCSA** and magnesium acetate in THF.[24] For the sake of a deep insight of the **BCSA**-Mg^{2+} interaction, these crystals were analyzed by single crystal X-ray diffraction. As illustrated in Fig. 6, the crystal structure of **BCSA**-Mg^{2+} contains one unique

Mg^{2+} center, two independent **BCSA** and two coordinated water molecules, which is in accordance with the conclusion deduced by Job's plot and ESI mass spectra. Moreover, the Mg^{2+} atom is six-coordinated in the form of a slightly distorted octahedron by four O atoms from two bidentate **BCSA** anion ligands with cis-configuration and two O atoms from two coordinated water molecules. These crystallographic data produce solid evidence and confirm the ^1H NMR data obtained in solution.

For the purpose of throwing light upon the mechanisms of the fluorescence signal changes for Mg^{2+} sensing as mentioned above, quantum calculations were carried out with the assist of Gaussian09_B.01 package, [25] involving the natural transition orbital (NTO)[26] analysis on the excited states (Fig. 7a). Compared to the familiar frontier molecular orbital (FMO) analyzing method, the NTO analyzing directly considers the real transition patterns in the excited states, instead of the base states, which is more persuasive in describing the characteristics of the excited states. As shown in Fig 7, from the NTO "Hole" to the "Particle", π-electrons of the excited states underwent a transition between 3, 5-position chlorine atoms and aldehyde group for both **BCSA** and **BCSA**-Mg^{2+}. Furthermore, the calculated emission spectra of **BCSA** and **BCSA**-Mg^{2+} complex in gas phase were centered at 498 nm (2.49 eV) and 443 nm (2.80 eV), respectively. This agrees with the available experimental data (centered at 500 and 481 nm, respectively). Such a result could explain the appearance of Mg^{2+}-induced blue shift of the emission in the fluorescence spectra. In the DFT optimized lowest excited-state geometry of the enol form of **BCSA** (Fig. S8, ESI†), there is a free proton located between the carbonyl O and phenol O. This means that in the excited singlet state, **BCSA** is generally acidic and exists in its deprotonated form, leading to a large Stokes-shifted emission, which is in accordance with the discussion above.

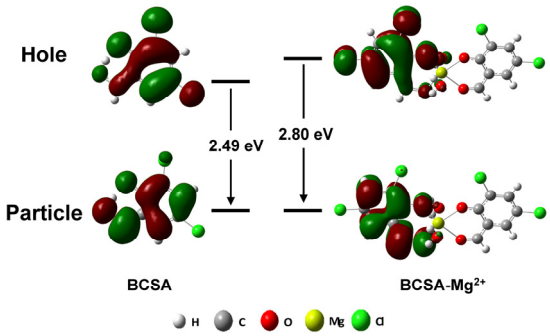

Fig. 7 $S_1 \rightarrow S_0$ natural transition orbital (NTO) and energy level diagram for the emissions of **BCSA** and **BCSA**-Mg^{2+} complex calculated by TD/DFT method. The NTO "Hole" and "Particle" represent the visualized wave functions of the excited molecules. The properties of the transition pattern illustrated above are both 99.9% according to the calculations.

Applications of the Mg^{2+} sensor and its PMMA thin film: Detecting in real samples from bottled drinking water.

The practical applications of the designed fluorescent chemosensor were first evaluated by detecting Mg^{2+} in real water samples from commercial bottled drinking water (obtained from three brands available in China), and the results were compared with those obtained from the standard EDTA titration method. According to the EDTA titration method, the concentration of Mg^{2+} may be calculated as the difference between hardness and calcium as $CaCO_3$ if suitable inhibitors are used in the hardness titration and interfering metals are present in non-interfering concentrations in the calcium titration. According to our proposed method, a 4.75 mL ethanol solution containing a spot of **BCSA** was added to the 0.25 mL HEPES buffer solution that was prepared by real water samples to keep the pH value at 7.0. As soon as the mixture solutions were prepared, we could easily observe their fluorescent color changes from green to light blue by naked eye, indicating the existance of Mg^{2+} in these real sample could be quickly determined. The details of the emission signal variations in these recognition systems were monitored by their fluorescence spectra (Fig. S9, ESI†). The data of the fluorescence intensity at 481 nm was fed back to the external calibration curve that was obtained above (Fig. 1b) and then the Mg^{2+} concentrations of the samples were obtained from this curve. All the measurements were performed three times. The analysis results summarized in Table 1 shows good agreement between the proposed optosensing method and the standard EDTA titration method for Mg^{2+} concentrations in real water samples with a relative error less than 2%. This indicates that the proposed sensor is applicable for real-time quantificational detection of Mg^{2+}; it can meet the sensitivity and selectivity requirements for practical applications involving the real water sample monitoring.

Table 1. Mg^{2+} concentrations found in different commercial drinking water samples.

	Sample 1	Sample 2	Sample 3
This method (mg/L)	4.91±0.12	3.78±0.09	1.67±0.05
Standard method (mg/L)	4.90±0.12	3.75±0.11	1.70±0.04
Relative error (%)	0.2	0.8	-1.8

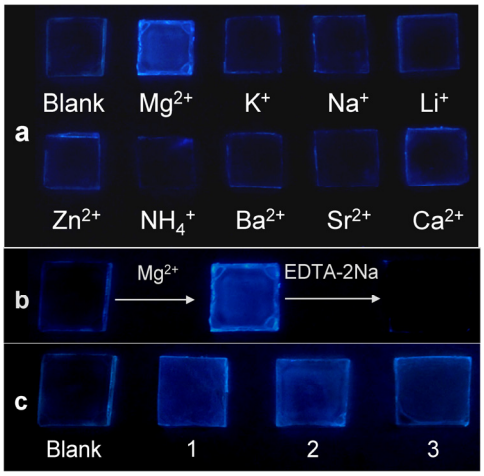

Fig. 8 (a) Fluorescence image of **BCSA**-doped PMMA sheets upon addition of different metal ions ([M] = 200 μM). (b) Fluorescence changes of **BCSA**-doped PMMA sheets toward Mg^{2+} and EDTA-2Na. (c) Fluorescence changes of **BCSA**-doped PMMA sheets toward three drinking water samples.

Functional material modified fluorescent dye probes are known for their great potential in being the environment monitoring device which can be convenient for applications in the future. So we were also devoted to the design and the fabrication of

polymeric thin film sensors for Mg^{2+}, using the PMMA thin film as the solid support to anchor the primary dye molecule **BCSA**.[27] This was expected to display the function of Mg^{2+} sensing. As shown in Fig. 8a, the unique highly blue fluorescent response toward Mg^{2+} demonstrated the high selectivity of this film. Furthermore, this film has been proved to be reusable according to the alternate immersion in the solutions containing Mg^{2+} and EDTA disodium, respectively (Fig. 8b). Finally, the films were dipped into the real samples from drinking water and rapidly dried in the oven. It can be observed from Fig. 8c that the fluorescence intensity of these films show evident enhancements. It means that this film sensor can also achieve the fast detection of Mg^{2+} in drinking water; therefore, it can reach its full potential in the area of portable field analysis.

Conclusions

In summary, we designed and developed an "off-the-shelf" fluorescence "turn-on" Mg^{2+} sensor **BCSA** that can be purchased from a commercial source without further synthesis. It works based on the Mg^{2+}-induced formation of 2:1 **BCSA**-Mg^{2+} complex, producing a chelation-enhanced fluorescence effect which has been studied by various spectroscopic methods involving fluorescence, UV-vis, ESI mass and NMR spectra. The binding mode of **BCSA** with Mg^{2+} was further confirmed by single crystal XRD analysis. We also used TD/DFT calculation to provide an in-depth explanation of the optical properties of the **BCSA** and **BCSA**-Mg^{2+}. In fluorescence spectra, addition of ~3 equiv. Mg^{2+} led to a significant quantum yield enhancement from 0.018 to 0.333 and a 22-fold fluorescence peak intensity enhancement. Over a wide Mg^{2+} concentration range (0-40 μM), **BCSA** can quantitatively detect Mg^{2+} with a low detection limit of 2.89×10^{-7} mol/L. It can also accomplish the real-time monitoring of Mg^{2+} with a short response time of less than 0.5 s. Moreover, **BCSA** shows an excellent selectivity toward Mg^{2+} over other common metal ions in drinking water. As a result, this proposed sensor **BCSA** can be utilized for the quantitative detection of Mg^{2+} in real water samples from bottled drinking water. For the convenience of the utilization in the future, **BCSA** was doped into the PMMA film to fabricate one kind of new Mg^{2+} polymeric thin film sensor. It was demonstrated to be a smart portable device which could respond reversibly to Mg^{2+} in drinking water with high selectivity.

Experimental section

Materials

All the materials for synthesis and spectra were purchased from commercial suppliers (analytical grade) and used without further purification. Solutions of metal ions were prepared from the corresponding hydrochloride. The solvents were HPLC grade (> 99%, Tianjin Guangfu Fine Chemical Research Institute) and dried over molecular sieves prior to use. Ultrapure water (18.25 MΩ*cm) from a Millipore Milli-Q purification system was used throughout the work. The three bottled drinking water samples are Wahaha natural mineral drinking water, Shengshuang mineral water and Quanyang Spring drinking water, respectively, which were purchased from commercial resources and used without further purification.

Instrumentation

The UV-vis absorption spectra were taken on a Shimadzu 3100 UV-VIS-NIR recording spectrophotometer using a 3 nm slit width. The fluorescence spectra were determined with a Shimadzu RF-5301PC spectrofluorophotometer. ^{1}H-NMR (TMS) and ^{13}C-NMR were recorded on a Bruker UltraShield 500MHz spectrometer. Mass spectra were measured on a Thermo Scientific ITQ 1100™ GC/MSn and a Q Trap MS (Applied Biosystems/MDS Sciex, Concord, ON, Canada) which was equipped with an electrospray ionisation (ESI) source. Elemental analyses were carried out with a vario MICRO cube elementar. Unless otherwise mentioned, all the measurements were performed at room temperature and repeated at least once.

Spectral measurements

Stock solutions of the metal ions (10 mM) were prepared in deionized water. A stock solution of **BCSA** (2 mM) was prepared in ethanol. The solution of **BCSA** was then diluted to 50 μM with a 95:5 (v/v) ethanol-HEPES buffer solution. In titration experiments, each time a 2 mL solution of **BCSA** (50 μM) was filled in a quartz optical cell of 1 cm optical path length, and the Mg^{2+} stock solution was added into the quartz optical cell gradually by using a micro-pipette. Spectral data were recorded at 2 min after the addition. In selectivity experiments, the test samples were prepared by placing appropriate amounts of metal ion stock into 2 mL solution of **BCSA** (50 μM). For fluorescence measurements, excitation was provided at 400 nm, and emission was collected from 403 to 625 nm.

Quantum yield measurement

The quantum yield is measured at room temperature by a single excitation wavelength (370 nm, which is coming from the Xenon lamp of the spectrofluorophotometer) referenced to quinine sulfate in sulfuric acid aqueous solution (3×10^{-5} mol/L quinine sulfate and 0.5 mol/L sulphuric acid, Φ_{fr} = 0.546) and calculated according to the equation as follow,[17d, 28] where Φ_{fs} is the radiative quantum yield of the sample; Φ_{fr} is the radiative quantum yield of the standard; A_s and A_r are the absorbances of the sample and standard at the excitation wavelength, respectively; D_s and D_r are the integrated areas of the emission for sample and standard, respectively; L_s and L_r are the lengths of the absorption cells for the sample and standard test; and N_s and N_r are the indexes of refraction of the sample and standard solutions (pure solvents were assumed), respectively.

$$\Phi_{fs} = \Phi_{fr} \times \frac{1-10^{-ArLr}}{1-10^{-AsLs}} \times \frac{N_s^2}{N_r^2} \times \frac{D_s^2}{D_r^2}$$

Preparation of the polymeric thin films

100 mg of the polymethylmethacrylate PMMA polymer (Mw = 12000, Sigma-Aldrich) was dissolved in dichloromethane (100 mL) and doped with **BCSA** (1 mM). The solution was poured onto a clean glass surface and a homogeneous, non-fluorescent polymer sensor film was obtained via spin-coating. This thin film

was used for Mg^{2+} detection. For the erasing process, a solution of EDTA disodium was sprayed onto the film after the film was dipped into real samples and dried. The non-fluorescent thin film was restored.

Synthesis of BCMB

An excess of freshly distilled methyl iodide was dropped in the DMF (15 mL) solution of 0.1 g **BCSA** with 0.072 g K_2CO_3. The mixture was stirred at 50 ℃ for 14 hours. The entire reaction mixture was then poured into water (50 mL) and extracted with diethyl ether (3 × 50 mL). All the organic extracts were collected and washed with 0.1 N NaOH solution (2 × 25 mL) followed by water (50 mL). The organic layer was dried over anhyd. Na_2SO_4 and evaporated to dryness. It was further purified by column chromatography on silica gel. A white, crystalline solid was obtained (68% yield). ^{1}H NMR (500 MHz, DMSO-d_6): δ 10.20 (s, 1H), 8.05 (d, J = 2.60 Hz, 1H), 7.70 (d, J = 2.60 Hz, 1H), 3.96 (s, 3H). MS: m/z calculated for $C_8H_6Cl_2O_2$ [M^+]: 203.97, found 203.93. Elemental analysis calculated for $C_8H_6Cl_2O_2$: C, 46.86; H, 2.95. Found: C, 47.15; H, 3.34.

Acknowledgements

This work was supported by the National Basic Research Program of China (2012CB933800) and the National Natural Science Foundation of China (21374036).

Notes and references

State Key Laboratory of Supramolecular Structure and Materials, Jilin University, 2699 Qianjin Avenue, Changchun, 130012, P. R. China. E-mail: smjiang@jlu.edu.cn; Fax: +86-431-85193421; Tel: +86-431-85168474.

†Electronic Supplementary Information (ESI) available: Characterization data of the compound **BCSA**, detailed properties for Mg^{2+} detection and other additional data. (Fig. S1-S9, Table S1). CCDC 950175. For ESI and other electronic format See. DOI: 10.1039/b000000x/

‡Crystal data for the compound **BCSA** ($C_{22}H_{26}Cl_4MgO_8$): M_w = 584.54, triclinic, space group: P-1, a = 10.477(2) Å, b = 11.673(2) Å, c = 12.937 (2) Å, α = 91.500(4)º, β = 106.143(3)º, γ = 115.291(3)º, V = 1354.8(3) Å^3, Z = 2, ρ_{calcd} = 1.433 Mg/m^3, μ(MoKα) = 0.503 mm^{-1}, F(000) = 604, T = 296(2) K, $2\theta_{max}$ = 56.44. 11157 reflections measured, of which 6618 were unique (R_{int} = 0.0251). Final R_1=0.0539 and wR_2=0.1456.

1 (a) M. J. Cromie, Y. X. Shi, T. Latifi and E. A. Groisman, Cell, 2006, 125, 71-84; (b) G. Farruggia, S. Lotti, L. Prodi, M. Montalti, N. Zaccheroni, P. B. Savage, V. Trapani, P. Sale and F. I. Wolf, J. Am. Chem. Soc., 2006, 128, 344-350; (c) L. Jin, Z. J. Guo, Z.Y. Sun, A. L. Li, Q. Jin and M. Wei, Sens. Actuators, B, 2012, 161, 714-720; (d) D. Ray, A. Nag, A. Jana, D. Goswami and P. K. Bharadwaj, Inorganica Chimica Acta, 2010, 363, 2824-2832.

2 (a) B. O'Rourke, P. H. Backx and E. Marban, Science, 1992, 257, 245; (b) C. Schmitz, A. Perraud, C. O. Johnson, K. Inabe, M. K. Smith, R. Penner, T. Kurosaki, A. Feig and A. M. Scharenberg, Cell, 2003, 113, 191; (c) Y. Zhao, A. M. Ren, L. Y. Zou, J. F. Guo and J. K. Feng, Theor. Chem. Acc., 2011, 130, 61-68; (d) S. Ishijima, A. Uchibori, H. Takagi, R. Maki and M. Ohnishi, Archives of Biochemistry and Biophysics, 2003, 412, 126-132.

3 (a) V. K. Gupta, R. Prasad and A. Kumar, Talanta, 2004, 63, 1027-1033.

4 (a) Y. Suzuki, H. Komatsu, T. Ikeda, N. Saito, S. Araki, D. Citterio, H. Hisamoto, Y. Kitamura, T. Kubota, J. Nakagawa, K. Oka and K. Suzuki, Anal. Chem. 2002, 74, 1423-1428; (b) T. Shoda, K. Kikuchi, H. Kojima, Y. Urano, H. Komatsu, K. Suzuki and T. Nagano, Analyst, 2003, 128, 719-723.

5 (a) M. Rosenlund, N. Berglind, J. Hallqvist, T. Bellander and G. Bluhm, Epidemiology, 2005, 16, 570-576; (b) A. Rosanoff, Medical Hypotheses, 2013, 81, 1063-1065.

6 T. M. Lerga and C. K. O'Sullivan, Anal. Chim. Acta, 2008, 610, 105-111.

7 (a) Standard Methods for the Examination of Water and Wastewater, American Public Health Association, 21th ed., 2005, Method 2340 C and Method 3500-Mg B; (b) R. A. C. Lima, S. R. B. Santos, R. S. Costa, G. P. S. Marcone, R. S. Honorato, V. B. Nascimento and M. C. U. Araujo, Anal. Chim. Acta, 2004, 518, 25-30.

8 (a) D. T. Quang and J. S. Kim, Chem. Rev., 2010, 110, 6280-6301. (b) D. G. Cho and J. L. Sessler, Chem. Soc. Rev., 2009, 38, 1647. (c) X. Q. Chen, Y. Zhou, X. J. Peng and J. Y. Yoon, Chem. Soc. Rev., 2010, 39, 2120. (d) Z. C. Xu, X. Q. Chen, H. N. Kim and J. Y. Yoon, Chem. Soc. Rev., 2010, 39, 127. (e) X. Q. Chen, X. Z. Tian, I. Shin and J. Y. Yoon, Chem. Soc. Rev., 2011, 40, 4783. (f) G. J. Mohr, Chem. Eur. J., 2004, 10, 1082.

9 (a) X. Q. Chen, T. Pradhan, F. Wang, J. S. Kim and J. Y. Joon, Chem. Rev. 2012, 112, 1910-1956. (b) Y. W. Liu, C. H. Chen and A. T. Wu, Analyst, 2012, 137, 5201.

10 (a) E. M. Nolan and S. J. Lippard, Chem. Rev., 2008, 108, 3443–3480; (b) H. S. Jung, P. S. Kwon, J. W. Lee, J. Kim, C. S. Hong, J. W. Kim, S. h. Yan, J. Y. Lee, J. H. Lee, T. Joo and J. S. Kim, J. Am. Chem. Soc., 2009, 131, 2008–2012; (c) D. W. Domaille, L. Zeng and C. J. Chang, J. Am. Chem. Soc., 2010, 132, 1194-1195; (d) Z. C. Xu, J. Y. Yoon and D. R. Spring, Chem. Soc. Rev., 2010, 39, 1996-2006.

11 (a) V. Trapani, G. Farruggia, C. Marraccini, S. Iotti, A. Cittadini and F. I. Wolf, Analyst, 2010, 135, 1855-1866; (b) H. Komatsu, T. Miki, D. Citterio, T. Kubota, Y. Shindo, Y. Kitamura, K. Oka and K. Suzuki, J. Am. Chem. Soc., 2005, 127, 10798-10799; (c) J. Brandel, M. Sairenji, K. Ichikawa and T. Nabeshima, Chem. Commun., 2010, 46, 3958-3960; (d) H. M. Kim, P. R. Yang, M. S. Seo, J. S. Yi, J. H. Hong, S. J. Jeon, Y. G. Ko, K. J. Lee and B. R. Cho, J. Org. Chem., 2007, 72, 2088-2096; (e) E. Brunet, M. T. Alonso, O. Juanes, R. Sedano and J. C. Rodríguez-Ubis, Tetrahedron Letters, 1997, 38, 4459-4462; (f) M. Suresh and A. Das, Tetrahedron Letters, 2009, 50, 5808-5812.

12 (a) S. H. Mashraqui, S. Sundaram, A. C. Bhasikuttan, S. Kapoor and A. V. Sapre, Sensors and Actuators B, 2007, 122, 347-350; (b) E. J. Shin, Chemistry Letters, 2002, 686-687.

13 J. Kim, T. Morozumi and H. Nakamura, Org. Lett., 2007, 9, 4419-4422.

14 (a) A. Hamdi, S. H. Kim, R. Abidi, P. Thuéry, J. S. Kim and J. Vicens, Tetrahedron, 2009, 65, 2818-2823; (b) K. C. Song, M. G. Choi, D. H. Ryu, K. N. Kim and S. K. Chang, Tetrahedron Letters, 2007, 48, 5397-5400.

15 (a) Y. Y. Ma, H. Liu, S. P. Liu and R. Yang, Analyst, 2012, 137, 2313; (b) N. Singh, N. Kaur, R. C. Mulrooney and J. F. Callan, Tetrahedron Letters, 2008, 49, 6690-6692; (c) L. N. Wang, W. W, Qin, X. L. Tang, W. Dou, and W. S. Liu, J. Phys. Chem. A, 2011, 115, 1609-1616; (d) D. Ray and P. K. Bharadwaj, Inorg. Chem. 2008, 47, 2252-2254.

16 P. Bühlmann, E. Pretsch and E. Bakker, Chem. Rev., 1998, 98, 1593-1687.

17 (a) G. W. Men, G. R. Zhang, C. S. Liang, H. L. Liu, B. Yang, Y. Y. Pan, Z. Y. Wang and S. M. Jiang, Analyst, 2013, 138, 2847-2857; (b) S. C. Wang, G. W. Men, L. Y. Zhao, Q. F. Hou and S. M. Jiang, Sensors and Actuators B, 2010, 145, 826-831; (c) L. B. Zang, D. Y. Wei, S. C. Wang and S. M. Jiang, Tetrahedron, 2012, 68,636-641; (d) L. Y. Zhao, D. Sui, J. Chai, Y. Wang and S. M. Jiang, J. Phys. Chem. B, 2006, 110, 24299-24304; (e) L. Y. Zhao, S. C. Wang, Y. Wu, Q. F. Hou, Y. Wang and S. M. Jiang, J. Phys. Chem. C, 2007, 111, 18387-18391.

18 (a) C. Godoy-Alcántar, A. K. Yatsimirsky and J. M. Lehn, J. Phys. Org. Chem., 2005, 18, 979-985; (b) I. Król-Starzomska, A. Filarowski, M. Rospenk and A. Koll, J. Phys. Chem. A, 2004, 108, 2131-2138.

19 (a) S. Nagaoka, N. Hirota, M. Sumitani and K. Yoshihara, J. Am. Chem. Soc., 1983, 105, 4220-4226; (b) S. Nagaoka, N. Hirota, M. Sumitani, K. Yoshihara, E. Lipczynska-Kochany and H. Iwamura, J. Am. Chem. Soc., 1984, 106, 6913-6916.
20 L. Stryer, J. Am. Chem. Soc., 1966, 88, 5708-5712.
21 (a) P. Chowdhury, S. Panja and S. Chakravorti, J. Phys. Chem. A, 2003, 107, 83-90; (b) T. Nishiya, S. Yamauchi, N. Hirota, Y. Fujiwara and M. Itoh, J. Am. Chem. Soc., 1986, 108, 3880-3884.
22 C. H. Chen, D. J. Liao, C. F. Wan and A. T. Wu, Analyst, 2013, 138, 2527.
23 (a) C. S. He, W. P. Zhu, Y. F. Xu, T. Chen and X. H. Qian, Analytica Chimica Acta, 2009, 651, 227-233; (b) H.M.N.H. Irving, H. Freiser, T.S. West, IUPAC Compendium of Analytical Nomenclature, Definitive Rules, Pergamon Press, Oxford, 1981.
24 (a) A. Erxleben and D. Schumacher, Eur. J. Inorg. Chem., 2001, 3039-3046; (b) Y. Watanabe, Y. Aritake and T. Akitsu, Acta Cryst., 2009, E65, m1640-m1641.
25 M. J. Frisch, G. W. Trucks et.al. Gaussian 09_B.01, Gaussian, Inc., Wallingford, CT, USA 2009.
26 R. L. Martin, J. Chem. Phys., 2003, 118, 4775.
27 C. Kaewtong, B. Wanno, Y. Uppa, N. Morakot, B. Pulpokac and T. Tuntulani, Dalton Trans., 2011, 40, 12578.
28 J. N. Demas and G. A. Grosby, J. Phys. Chem. 1971, 75, 991-1024.